COMMUNICATIONS PHYSICS

ARTICLE

https://doi.org/10.1038/s42005-020-0321-7 OPEN

Sub-cycle coherent control of ionic dynamics via transient ionization injection

Qian Zhang[1,6], Hongqiang Xie[1,2,6], Guihua Li[1,3], Xiaowei Wang[1], Hongbin Lei[1], Jing Zhao[1], Zhiming Chen[2], Jinping Yao[4], Ya Cheng[5] & Zengxiu Zhao[1]✉

Ultrafast ionization of atoms or molecules by intense laser pulses creates extremely non-stationary ionic states. This process triggers attosecond correlated electron-hole dynamics and subsequent ultrafast non-equilibrium evolution of matters. Here we investigate the interwoven dynamic evolutions of neutral nitrogen molecules together with nitrogen ions created through transient tunnel ionization in an intense laser field. Based on the proposed theoretical frame, it is found that nitrogen molecular ions are primarily populated in the electronically excited states, rather than staying in the ground state as predicted by the well-known tunneling theory. The unexpected result is attributed to sub-cycle switch-on of time-dependent polarization by transient ionization and dynamic Stark shift mediated near-resonant multiphoton transitions. These findings corroborate the mechanism of nitrogen molecular ion lasing and are likely to be universal. The present work opens a route to explore the important role of transient ionization injection in strong-field induced non-equilibrium dynamics.

[1] Department of Physics, National University of Defense Technology, Changsha 410073, China. [2] State Key Laboratory of Nuclear Resources and Environment, East China University of Technology, Nanchang 330013, China. [3] School of Science, East China Jiaotong University, Nanchang 330013, China. [4] State Key Laboratory of High Field Laser Physics, Shanghai Institute of Optics and Fine Mechanics, Chinese Academy of Sciences, Shanghai 201800, China. [5] State Key Laboratory of Precision Spectroscopy, East China Normal University, Shanghai 200062, China. [6] These authors contributed equally: Qian Zhang, Hongqiang Xie ✉email: zhaozengxiu@nudt.edu.cn

The fundamental process of strong-field ionization of atoms by intense ultrashort laser pulses occurs at attosecond timescale[1–3] and lasts for pulse lengths in femtoseconds. The temporal confined strong field ionization (SFI) creates broad bandwidth non-stationary ionic states along with the launching of attosecond electron wavepacket forming the foundation of attosecond physics[4–8]. One of the key problem is how the coherence of the ionic states affect the subsequent ultrafast non-equilibrium evolution ranging from charge migration in molecules[9], electron transport in condense matter[10] to ultrafast laser processing of materials[11]. It is particular intriguing to question whether the further interaction of the ions with lasers can be considered independently by assuming the prior ionization is completed?

Recent experiments indicate that the interplay of sub-cycle SFI and the followed ion-laser coupling is indispensable for nitrogen molecular ion lasing[12–16], which suggests the new possibility to manipulate the ion coherence upon its creation toward ion-based quantum optics. While SFI itself can be described well by the celebrated Keldysh tunneling theory[17], a complete model treating both ionization of neutrals and laser-ion couplings on the equal footing is still lacking. Theoretically, dealing with bounded multi-electron problem is already a difficult task, it is even challenging for open quantum many-body systems when ionization is involved. Exact time-dependent multilelectron theories are limited to two electrons cases[18] or struggling with ionization-induced derivative discontinuities in density-functionals[19]. A lot of theoretical works have devoted to the coherent ionic evolution in a multi-channel formalism[20–24] but the ion-laser coupling within the ionization process remains elusive.

Considering the ionization of nitrogen molecules by intense laser pulses. As illustrated in Fig. 1, ionization creates the ion in three possible electronic states at the moment t_i by releasing the electron, the remaining linearly polarized laser field will further induce coherence and population transfer among the electronic and vibrational states with the couplings depending on the geometry of the molecular ion. According to the tunneling ionization theory[17,25], the population on the excited ionic states is expected to be much less than that on the ionic ground state. However, due to the continuous presence of the laser field, the ions created by SFI will be polarized by the laser field[26] causing the electron to oscillate back and forth between electronic states.

In the present work, by treating nitrogen molecules as an open quantum system, we systematically investigate the role of transient injection of ions by SFI on ultrafast population redistribution of ionic states. As we will demonstrate, the sub-cycle turn-on of the polarization of the ion upon its creation breaks the time-reversal symmetry and it is thus possible to enhance the population on the higher excited states. Furthermore, in the case of resonance, the population on the excited states can also be greatly increased by multiphoton couplings mediated by dynamic Stark shift due to the instantaneous polarization. The ultrafast population redistribution of electronic states of molecular ions assisted by transient ionization might be a universal process for other molecular ionization from multiple orbitals and bond breaking and thus SFI can serve as an intrinsic attosecond probe to the sub-cycle ionic coherence. Our finding sheds more light on the SFI-coupling mechanism and provides crucial implications for further research on coherent emissions from molecular ions.

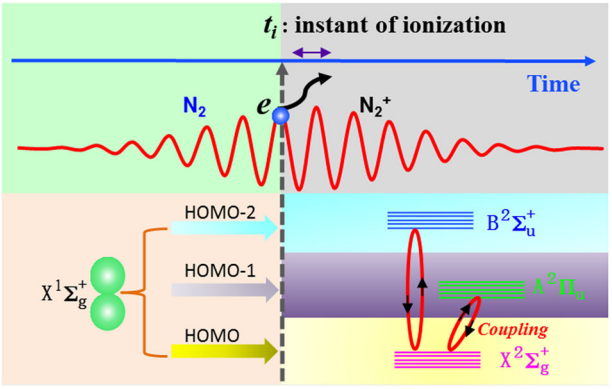

Fig. 1 Transient ionization-coupling model. Illustration of the dynamic processes of nitrogen molecules in an intense laser pulse. Strong field ionization injects the ions into three possible electronic states that are driven by the remaining laser pulse. Note that the X-B transition is parallel and X-A transition is perpendicular to the molecular axis. HOMO highest occupied molecular orbital.

Results

Population inversion and vibrational redistribution. We now present our results, which are obtained by solving the ionization-coupling model in the methods section. The details of calculation can be found in Supplementary Notes 1 and 2. We first discuss the nitrogen molecule whose axis is aligned to be 45° with respect to the pump laser polarization and therefore both the transitions of X-A, X-B are permitted. The rotational degree of freedom is assumed to be frozen in the present work. The solid curves in Fig. 2a shows the population evolution of the three electronic states of N_2^+ in the pump laser field by solving ionization-coupling equation. It can be clearly seen that the final populations on the states A and B are prominently increased while that on the state X is greatly decreased in comparison to the case that only ionization is considered (the dashed curves in Fig. 2a). It can be seen that with the help of the transient injection the population between the states B and X is thus inverted. This is striking in view of that other processes, e.g, shake-up[27,28] or recollision[29,30] are unlikely to produce ionic population inversion.

The vibrational state-resolved distributions for each electronic state are respectively displayed in Fig. 2b–d. As can be seen, for the electronic state X, the ionization itself mainly populates the vibrational states $v = 0$, 1 because of the relatively larger Franck–Condon factors of the two states[31]. However, when the coupling is incorporated, the vibrational population on the state $v = 0$ is largely reduced while higher vibrational states are more populated. It can be attributed to vibrational Raman-like processes when a strong coherent coupling is produced between the states X and A. As a consequence of the X state population reduction, almost all the vibrational population on the state A are efficiently enhanced due to one-photon X-A resonant transition. Remarkably, the vibrational-state population on the state B (especially for $v = 0$) are considerably increased as well although the laser frequency is far off from X-B resonant energy. Note that the vibrational energy gap between the states $A(v = 0–4)$ and X $(v = 0)$ spans from 1.12 to 2.06 eV and the driving laser photon energy ranges from 1.38 to 1.77 eV (700–900 nm). For the excited state $B(v = 0–4)$, the vibrational energy differences with respect to the ground state $X(v = 0)$ are in the range of 3.17–4.37 eV. The population transfer from the state $X(v = 0)$ is only accessible to high vibrational states $B(v = 3, 4)$ through a direct three-photon coupling.

Sub-cycle control of laser-ion coupling via transient ionization injection. In order to better understand the observed population enhancement of the lower vibrational states (i.e., $v = 0$, 1, 2) of the state B, we fixed nitrogen molecular axis to be parallel to the laser polarization, by which the A-X coupling is avoided. In the following, we mainly focus on the B $(v = 0)$ state because the

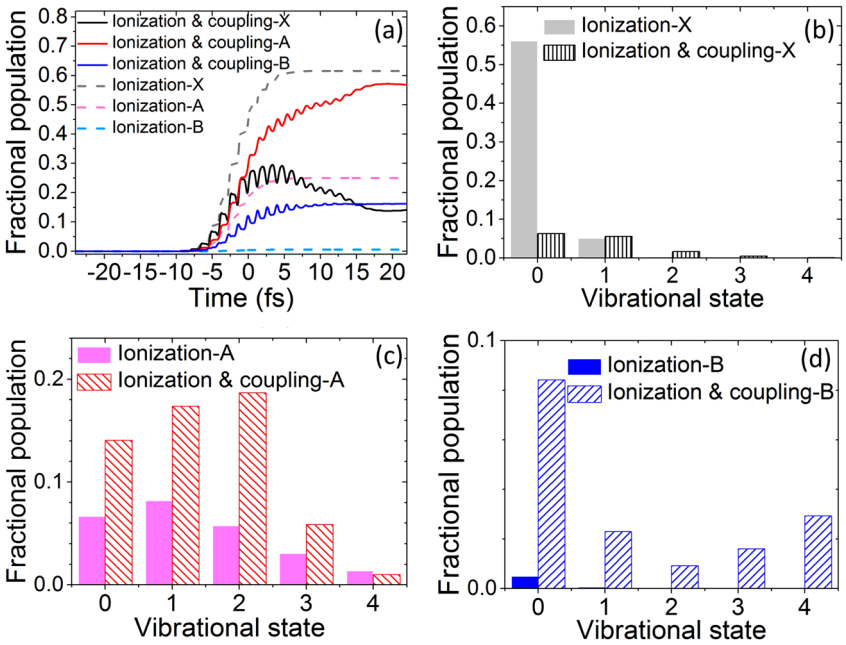

Fig. 2 Ionic population distribution with and without the coupling process. a Dynamic evolution of electronic state population of N_2^+ taking into account of both ionization and laser-ion coupling (solid curves), and that obtained by considering only the ionization (dashed curves). The molecular axis is aligned to be 45° with respect to the laser polarization direction. The final vibrational state-resolved population distribution for each electronic state after interaction are respectively shown in **b**–**d**.

manipulation of its population is critical to air lasing at 391 nm[12,14,15,32–35].

Figure 3a shows the evolution of the vibrational population of the ionic states $B(v=0)$ and $X(v=0)$ for the parallel alignment case. Again, the population on the state $B(v=0)$ is apparently promoted with the aid of simultaneous ionization and coupling. To investigate the influence brought by ionization on the coupling between $B(v=0)$ and $X(v=0)$, we first consider the ionization injection at the peak laser intensity and then follow the evolution of the ions in the second half of the laser field $E(t) = f(t)\cos(\omega t+\phi)$ with different phase ϕ. The corresponding laser fields for $\phi=0$, $\pi/4$, $\pi/2$ are respectively depicted in the top portion of the Fig. 3b. The injection is all populated on the ground state X of N_2^+, i.e., $\rho_{XX}^{+}(v=0)=1$. Figure 3b plots the final population of the state $B(v=0)$ as a function of the initial phase ϕ for the pump wavelength 800 nm. Interestingly, the obtained population on the state $B(v=0)$ is strongly modulated with a period of π and the maximum value is achieved at $\phi=0$. This explains that the yield population calculated in[13] who chose $\phi=\pi/2$ is less than that calculated in[12] who chose $\phi=0$ using their three-state coupling model.

We now consider how the coupling varies with the field profile assuming the ionization injection occurs at the peak field of each optical cycle (corresponding to fixed $\phi=0$). The population on the $B(v=0)$ and $X(v=0)$ states of N_2^+ after the laser-ion coupling are shown in Fig. 3c as a function of the instant of transient ionization injection. The yield population on the state $B(v=0)$ shows a nearly Gaussian dependence on the moments of ionization injection following the intensity profile of the pumping laser, as depicted by the black squares Fig. 3c. The stronger of transient electric fields at the injection of the ground-state ions, the more population on the state $B(v=0)$ and reversely the less population on the state $X(v=0)$ are found after the pulse is finished.

Multiphoton transition mediated by dynamic Stark shift. Further enhancement of the population on the state $B(v=0)$ can be achieved by resonant transitions from $X(v=0)$. Since this process is sensitive to the central wavelength of laser pulses, we calculated the population dependence on the driving laser frequency by solving ionization-coupling equation. As shown in Fig. 4a, a three-photon resonant peak for $B(v=0)$ appears at the wavelength of 900 nm, which deviates from the field-free three-photon resonant wavelength (1173 nm). Additional resonant peak around 1560 nm belongs to five-photon resonance. Figure 4b shows the corresponding frequencies of the two resonant peaks as a function of the peak intensity of the driving laser field. Both three-photon and five-photon resonant peaks exhibit a linear dependence on the peak intensity of the laser field. Surprisingly, the shift of the resonance is independent of the driving frequency, which can be attributed to the Stark shift by instantaneous polarization of the laser coupled X and B state at the instant of ionization injection.

Figure 4c shows the sub-cycle control of the population on the state $B(v=0)$ by changing the envelope phase ϕ at the resonant wavelength of 900 nm. It can be seen that the population on the state $B(v=0)$ is also modulated with a period of π. However, the maximum value is no longer at $\phi=0$ and the minimum value is not reached at $\phi=\pi/2$, which signifies that the polarization mechanism is not dominating in the case of resonance. The irregular modulation (black circles) indicates that a multi-channel interference might contribute to the population increment of the state $B(v=0)$. Figure 4d shows the dependence of the population yields on the injection time. A striking difference with the results in Fig. 3c is that in the case of resonance, the population on the state $B(v=0)$ is closely related to the post-ionization interaction time. The population on the state $B(v=0)$ shows a gradual decay with decreasing coupling time in the current conditions. It should be noted that the three-photon resonant transfer from $X(v=0)$ to $B(v=0)$ at a resonant wavelength is taking place during the evolution of the quantum coherent system driven by ultrafast polarization. Therefore the population increment of the state $B(v=0)$ should originate from the two-channel interference, i.e., polarization and three-photon resonant coupling.

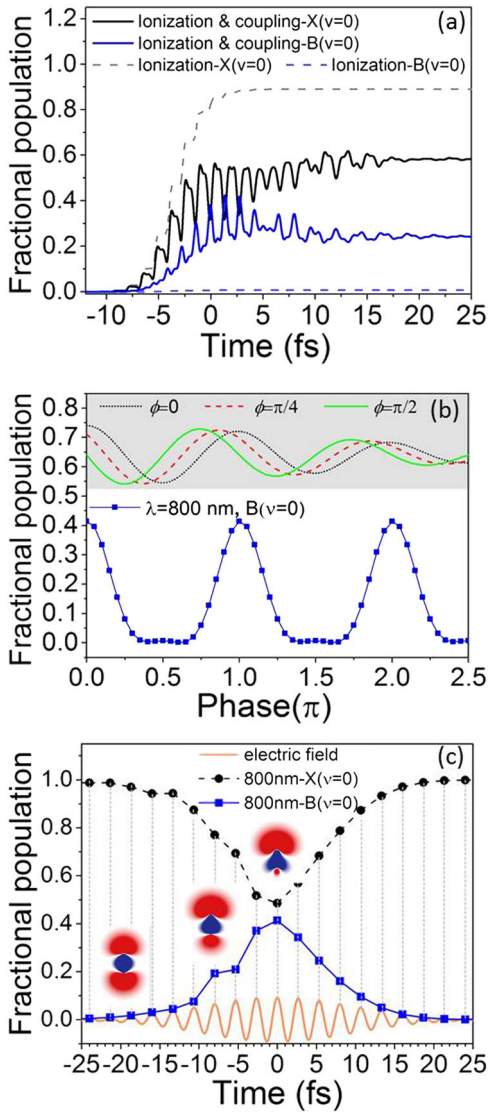

Fig. 3 Coherent manipulation of ionic population by subcycle ionization injection. a Dynamic evolution of electronic state populations of N_2^+ when the molecular axis is parallel to the laser polarization. **b** Variation of $B(v = 0)$ population with the initial injection phase ϕ after interacting with a half laser pulse at 800 nm. The corresponding laser fields as functions of time for $\phi = 0$, $\pi/4$, $\pi/2$ are respectively depicted. **c** dependence of the yield population on the injection instants within the full laser pulse. At these instants, the laser field takes local maximum at each individual optical cycle. The contour plot illustrates the transient ionic states that are polarized according to the instantaneous laser field.

Discussions

The above results in Fig. 3 can be qualitatively explained with ultrafast polarization theory. At a particular time, nitrogen molecular ions are prepared by transient SFI, which can be regarded as an ultrafast pump for the ionic system. Immediately following SFI, the ion is polarized by the instantaneous laser field as illustrated by the contour plot shown in Fig. 3c.

Since the electronic states B and X forming a pair of charge resonance states, strong polarization could occur due to their coherent coupling in the residual laser field. For different injection instants of ionization, the polarization state of ions is different, resulting in different population increment of the state $B(v = 0)$. For the case in Fig. 3b, the probability for populating on the state $B(v = 0)$ is greatest at $\phi = 0$ while at $\phi = \pi/2$, the probability is smallest. For comparisons of different ionization injection moments at the same envelope phase in Fig. 3c, the final population on the state $B(v = 0)$ varies because the instantaneous polarizability is proportional to the transient electric field. Therefore, transient ionization injection acts as an ultrafast probe of a quantum coherent system consisting of the neutral and molecular ions. Note that we ignore the dynamic anti-screening due to the ionic core polarization[26] on the tunneling ionization from the valence shell electrons.

The injection of ionization can be considered as an ultrafast streaking of the laser-driven ionic dynamics analogy to the attosecond streaking and transient absorption techniques[4,5,5,36,37]. Achieving the experimental measurement analogy to attosecond streaking is a challenging and open problem due to the lacking of an attosecond pulse in the visible wavelength range. However, two approaches may be accessible to measure the transient injection-induced population on the B state. With the aid of high harmonic sources, the phase-dependent population on the X or B state can be detected by attosecond absorption spectroscopy based on the transitions from the X to C (i.e., $C^2\Sigma_u^+$) state or from the B to D (i.e., $D^2\Pi_g$) state. Another possible means is to measure the absorption spectroscopy from X to B state after compressing a 400 nm pulse to a few cycles in addition to the polarization gating technique[15,38]. The Fourier transformation of the phase-dependent populations on the state B in Fig. 4c quantitatively gives the relative contributions of multiple photon dressing, which is shown in Supplementary Fig. 1. A concrete analysis on this based on an analytic solution is given in Supplementary Note 2. It is worth mentioning that for the non-parallel alignment case, transient ionization could influence both the coupling of A-X and B-X, which is discussed in Supplementary Note 3. Last but not the least, in the current model, we have ignored the ionization delays while injection of ions and the coherence brought by ionization. A more complete calculation including these effects will be carried out in the future.

In conclusion, we have systematically investigated the coherent evolution of nitrogen molecular ions, which are continuously injected by transient SFI in an intense laser field. It is found that the population on the excited states of nitrogen molecular ion can be greatly increased due to transient-injection-induced collapse of a quantum system and resonant multiphoton couplings. Our findings provide crucial clues to create high-intensity air lasers using femtosecond laser pulses and highlight the importance of ionization-induced coherence. The proposed theoretical frame allows us to treat transient ionization and laser-ion coupling for open quantum systems under strong laser fields. It can be generalized to explore the important role of transient ionization injection in other strong-field induced non-equilibrium dynamics, e.g., localization of electrons during dissociative ionization and autoionization of molecules in intense laser pulses.

Methods

Strong field ionization-coupling equation for ionic dynamics. We consider tunnel ionization mainly from three N_2 molecular orbitals, i.e., HOMO (i.e., highest occupied molecular orbital), HOMO-1, and HOMO-2 in a linearly polarized pump laser field with the peak intensity of 3×10^{14} W cm^{-2}, pulse duration of 15 fs and the central wavelength of 800 nm. The ionization energies of these orbitals are respectively 15.6 eV, 17 eV and 18.8 eV[39]. The molecular Ammosov–Delone–Krainov (MO-ADK) theory is employed to calculate the transient ionization rates of the involved three orbitals[25]. Once the three ionic states $X^2\Sigma_g^+$ (i.e., X), $A^2\Pi_u$ (i.e., A) and $B^2\Sigma_u^+$ (i.e., B) are prepared at the moment of ionization, population couplings among them will take place in the residual laser field.

Considering both the transient ionization injection and coupling effects, the evolution of the ionic density matrix $\rho^+(t)$ in an intense laser field is given by

$$\frac{d(\rho^+)}{dt} = -\frac{i}{\hbar}[H_I(t), \rho^+(t)] + \left(\frac{d(\rho^+)}{dt}\right)_{ionization} \quad (1)$$

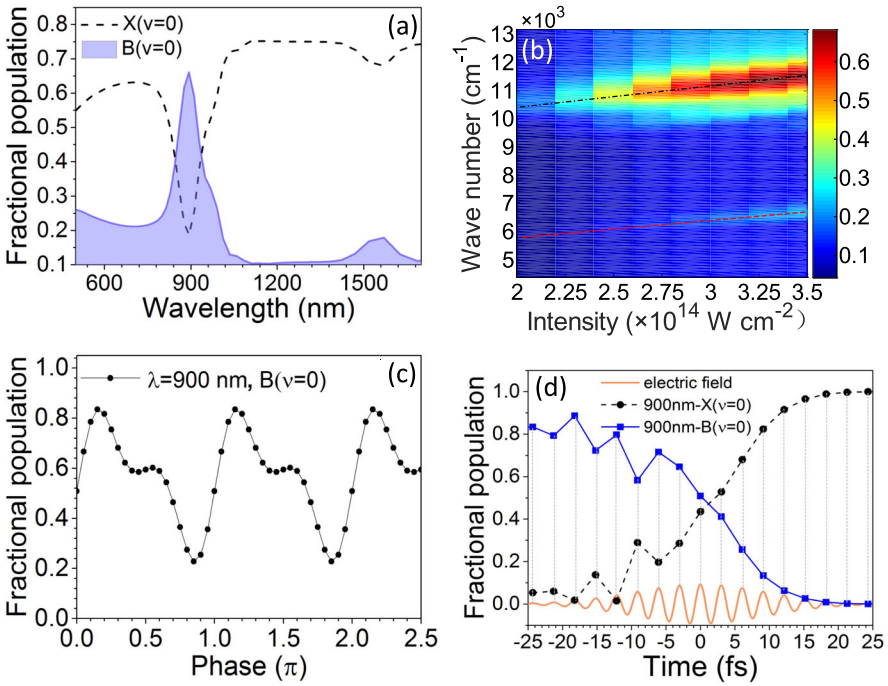

Fig. 4 Ionic population modulation considering Stark effect induced resonance. a Final population on the state $B(v=0)$ and $X(v=0)$ as a function of the central laser frequency. **b** Contour plot of the final population verse laser intensity and frequency. The three-photon and five-photon resonant frequencies shift with the applied laser peak intensity is indicated by the corresponding linear fittings (black dash-dotted and red dashed curves). **c** The dependence of $B(v=0)$ population on the initial injection phase ϕ at the central wavelength of 900 nm. **d** Dependence of $B(v=0)$ and $X(v=0)$ populations on the moments of ionization injection by fixing the carrier phase in the near-resonant case at the central wavelength of 900 nm.

where H_I is the ionic Hamiltonian in the interaction picture whose explicit form is provided in Supplementary Note 1. The last term in Eq. (1) describing the continuous injection of ions by transient ionization within the full laser pulse is one of the significant advances in this work. Its nondiagonal elements are assumed to be zero due to a vanishing coherence resulting from transient ionization and the diagonal elements are given by

$$\left(\frac{d(\rho_{iv}^{+})}{dt}\right)_{ionization} = \Gamma_{iv}(t)\rho_0 \qquad (2)$$

where $i = X, A, B$ labels the electronic states and $v = 0$–4 are the vibrational quantum numbers. The neutral population ρ_0 is decaying according to $\frac{d\rho_0}{dt} = -\sum\Gamma_{iv}\rho_0$ where $\Gamma_{iv}(t)$ are the ionization rates to the respective electronic-vibrational states. For the time being, the rotational states are unresolved and dissipation by collisions are ignored because of the short pulse duration.

Data availability

Simulation data and figures are available from Z.Z. upon reasonable requests.

Received: 30 November 2019; Accepted: 25 February 2020;
Published online: 12 March 2020

References

1. Eckle, P. et al. Attosecond ionization and tunneling delay time measurements in Helium. *Science* **322**, 1525–1529 (2008).
2. Schultze, M. et al. Delay in photoemission. *Science* **328**, 1658–1662 (2010).
3. Klünder, K. et al. Probing single-photon ionization on the attosecond time scale. *Phys. Rev. Lett.* **106**, 143002 (2011).
4. Goulielmakis, E. et al. Real-time observation of valence electron motion. *Nature* **466**, 739–743 (2010).
5. Wirth, A. et al. Synthesized light transients. *Science* **334**, 195–200 (2011).
6. Wörner, H. J. & Corkum, P. B. Imaging and controlling multielectron dynamics by laser-induced tunnel ionization. *J. Phys. B: At. Mol. Opt. Phys.* **44**, 041001 (2011).
7. Ossiander, M. et al. Attosecond correlation dynamics. *Nat. Phys.* **13**, 280–285 (2017).
8. Sabbar, M. et al. State-resolved attosecond reversible and irreversible dynamics in strong optical fields. *Nat. Phys.* **13**, 472–478 (2017).
9. Cederbaum, L. S. & Zobeley, J. Ultrafast charge migration by electron correlation. *Chem. Phys. Lett.* **307**, 205–210 (1999).
10. Cavalieri, A. L. et al. Attosecond spectroscopy in condensed matter. *Nature* **449**, 1029–1032 (2007).
11. Malinauskas, M. et al. Ultrafast laser processing of materials: from science to industry. *Light: Science & Applications* **5**, e16133 (2016).
12. Xu, H., Lötstedt, E., Iwasaki, A. & Yamanouchi, K. Sub-10-fs population inversion in N_2^+ in air lasing through multiple state coupling. *Nat. Comm.* **6**, 8347 (2015).
13. Yao, J. et al. Population redistribution among multiple electronic states of molecular nitrogen ions in strong laser fields. *Phys. Rev. Lett.* **116**, 143007 (2016).
14. Liu, Y. et al. Recollision-induced superradiance of ionized nitrogen molecules. *Phys. Rev. Lett.* **115**, 133203 (2015).
15. Li, H. et al. Significant enhancement of N_2^+ lasing by polarization-modulated ultrashort laser pulses. *Phys. Rev. Lett.* **122**, 013202 (2019).
16. Misyrowicz, A. et al. Lasing without population inversion in N_2^+. *APL Photon* **4**, 110807 (2019).
17. Keldysh, L. V. Ionization in the field of a stong electromagnetic wave. *Sov. Phys. JETP* **20**, 1307 (1965).
18. van der Hart, H. W., Lysaght, M. A. & Burke, P. G. Time-dependent multielectron dynamics of Ar in intense short laser pulses. *Phys. Rev. A* **76**, 043405 (2007).
19. Lein, M. & Kummel, S. Exact time-dependent exchange-correlation potentials for strong-field electron dynamics. *Phys. Rev. Lett.* **94**, 143003 (2005).
20. Santra, R., Dunford, R. W. & Young, L. Spin-orbit effect on strong field ionization of krypton. *Phys. Rev. A* **74**, 043403 (2006).
21. Rohringer, N. & Santra, R. Multichannel coherence in strong field ionization. *Phys. Rev. A* **79**, 053402 (2009).
22. Zhang, Y., Lötstedt, E. & Yamanouchi, K. Population inversion in a strongly driven two-level system at far-off resonance. *J. Phys. B: At. Mol. Opt. Phys.* **50**, 185603 (2017).
23. Zhang, Y., Lötstedt, E. & Yamanouchi, K. Mechanism of population inversion in laser-driven N_2^+. *J. Phys. B: At. Mol. Opt. Phys.* **52**, 055401 (2019).
24. Leth, H. A., Madsen, L. B. & Mølmer, K. Monte carlo wave packet theory of dissociative double ionization. *Phys. Rev. Lett.* **103**, 183601 (2009).
25. Tong, X. M., Zhao, Z. X. & Lin, C. D. Theory of molecular tunneling ionization. *Phys. Rev. A* **66**, 033402 (2002).

26. Zhang, B., Yuan, J. & Zhao, Z. Dynamic core polarization in strong-field ionization of CO molecules. *Phys. Rev. Lett.* **111**, 163001 (2013).
27. Litvinyuk, I. V. et al. Shakeup excitation during optical tunnel ionization. *Phys. Rev. Lett.* **94**, 033003 (2005).
28. Bryan, W. A. et al. Atomic excitation during recollision-free ultrafast multi-electron tunnel ionization. *Nat. Phys* **2**, 379–383 (2006).
29. Britton, M. et al. Testing the role of recollision in N_2^+ air lasing. *Phys. Rev. Lett.* **120**, 133208 (2018).
30. Li, H. et al. Air lasing from singly ionized N_2 driven by bicircular two-color fields. *Phys. Rev. A* **99**, 053413 (2019).
31. Alf, L. & Paul, H. K. The spectrum of molecular nitrogen. *J. Phys. Chem. Ref. Data* **6**, 113 (1977).
32. Yao, J. et al. High-brightness switchable multiwavelength remote laser in air. *Phys. Rev. A* **84**, 051802 (2011).
33. Xie, H. et al. Coupling of N_2^+ rotational states in an air laser from tunnel-ionized nitrogen molecules. *Phys. Rev. A* **90**, 042504 (2014).
34. Zhong, X. et al. Vibrational and electronic excitation of ionized nitrogen molecules in intense laser fields. *Phys. Rev. A* **96**, 043422 (2017).
35. Miao, Z. et al. Stimulated-Raman-scattering-assisted superfluorescence enhancement from ionized nitrogen molecules in 800-nm femtosecond laser fields. *Phys. Rev. A* **98**, 033402 (2018).
36. Itatani, J. et al. Attosecond streak camara. *Phys. Rev. Lett.* **88**, 173903 (2002).
37. Chini, M. et al. Subcycle ac stark shift of helium excited states probed with isolated attosecond pulses. *Phys. Rev. Lett.* **109**, 073601 (2012).
38. Xie, H. et al. Vibrational population transfer between electronic states of N_2^+ in polarization-modulated intense laser fields. *Phys. Rev. A* **100**, 053419 (2019).
39. Chong, D. P., Gritsenko, O. V. & Baerends, E. J. Interpretation of the Kohn-Sham orbital energies as approximate vertical ionization potentials. *J. Chem. Phys.* **116**, 1760 (2002).

Acknowledgements

This work is supported by China National Key R&D Program (Grant no. 2019YFA0307703), the Major Research plan of NSF (Grant no. 91850201), the National Natural Science Foundation of China (Grant nos. 61705034, 61605227 and 11704066) and Natural Science Foundation of Jiangxi Province (Grant no. 20171BAB211007), Science and Technology Project of Jiangxi Provincial Education Department (Grant nos. GJJ160587 and GJJ160576).

Author contributions

Z.Z. conceived the idea. Q.Z. did the numerical modeling and simulations under supervision by H.X. and Z.Z.. H.X. and Z.Z. prepared the paper. G.L., X.W., H.L., J.Z. and Z.C. participated in the discussions. J.Y. and Y.C. stimulated this work and reviewed the manuscript.

Competing interests

The authors declare no competing interests.

Additional information

Supplementary information is available for this paper at https://doi.org/10.1038/s42005-020-0321-7.

Correspondence and requests for materials should be addressed to Z.Z.

Reprints and permission information is available at http://www.nature.com/reprints

Publisher's note Springer Nature remains neutral with regard to jurisdictional claims in published maps and institutional affiliations.